HHS Public Access

Author manuscript

ACS Chem Biol. Author manuscript; available in PMC 2021 February 12.

Published in final edited form as:

ACS Chem Biol. 2016 July 15; 11(7): 1810–1815. doi:10.1021/acschembio.6b00233.

Profiling Esterases in *Mycobacterium tuberculosis* Using Far-Red Fluorogenic Substrates

Katie R. Tallman, **Samantha R. Levine**, **Kimberly E. Beatty***

Program in Chemical Biology and the Department of Biomedical Engineering, Oregon Health & Science University, Portland, Oregon 97201, United States

Abstract

Enzyme-activated, fluorogenic probes are powerful tools for studying bacterial pathogens, including *Mycobacterium tuberculosis* (*Mtb*). In prior work, we reported two 7-hydroxy-9*H*- (1,3-dichloro-9,9-dimethylacridin-2-one) (DDAO)-derived acetoxymethyl ether probes for esterase and lipase detection. Here, we report four-carbon (C4) and eight-carbon (C8) acyloxymethyl ether derivatives, which are longer-chain fluorogenic substrates. These new probes demonstrate greater stability and lipase reactivity than the two-carbon (C2) acetoxymethyl ether-masked substrates. We used these new C4 and C8 probes to profile esterases and lipases from *Mtb*. The C8-masked probes revealed a new esterase band in gel-resolved *Mtb* lysates that was not present in lysates from nonpathogenic *M. bovis* (bacillus Calmette-Guérin), a close genetic relative. We identified this *Mtb*-specific enzyme as the secreted esterase Culp1 (Rv1984c). Our C4- and C8-masked probes also produced distinct *Mtb* banding patterns in lysates from *Mtb*-infected macrophages, demonstrating the potential of these probes for detecting *Mtb* esterases that are active during infections.

Graphical Abstract

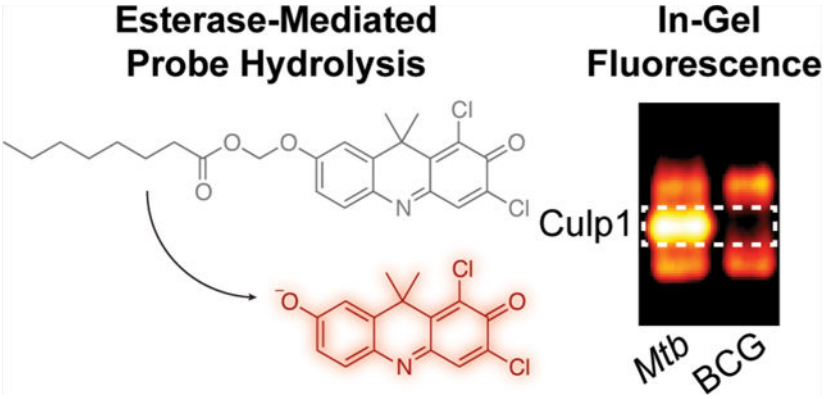

***Corresponding Author:** beattyk@ohsu.edu.

Supporting Information

The Supporting Information is available free of charge on the ACS Publications website at DOI: 10.1021/acschem-bio.6b00233. Details of synthetic procedures, regioisomer determination, enzymatic assays, cell culture conditions, and supporting figures and tables (PDF)

The authors declare no competing financial interest.

Mycobacterium tuberculosis (*Mtb*) is the causative agent of tuberculosis (TB), a major global health threat. In 2014, there were an estimated 9.6 million new cases and 1.5 million deaths from TB, making it the most lethal single-agent infectious disease.[1] After initial infection, *Mtb* can persist for decades as a latent, asymptomatic infection, with reactivation from dormancy occurring in approximately 10% of individuals.[2] In both latent and active TB, *Mtb* adapts to its environment by regulating enzyme activity, but hydrolase regulation in latency and the roles of these enzymes during reactivation are poorly understood. This is due, in part, to the scarcity of tools available to monitor and track hydrolase activities in complex samples (e.g., lysates and tissues).

Mtb utilizes host-derived lipids as an energy source during dormancy and reactivation, making lipid metabolizing enzymes attractive targets for new diagnostic biomarkers or therapeutics.[3–6] The importance of lipid metabolism for *Mtb* growth, persistence, and pathogenicity is reflected in the 250 *Mtb* genes linked to lipid processing—about 5 times as many as found in *E. coli*, which has a similarly sized genome.[7] Of these 250 genes, 21 were initially annotated as encoding esterases or lipases, a lipid-preferring subclass, but the actual number is likely at least 2-fold higher. Ninety-four gene products are predicted to contain the α/β hydrolase fold characteristic of these enzymes,[8] and misannotated esterases and lipases continue to be identified.[9–13] However, difficulties expressing and isolating active *Mtb* esterases and lipases have hindered *in vitro* characterization of these enzymes.[3,11,14]

To circumvent this challenge, we directly assessed *Mtb* hydrolase activities using an assay that combined fluorogenic probes with native polyacrylamide gel electrophoresis (PAGE)-resolved cellular lysates. Distinct hydrolases were detected in-gel by selecting an appropriate fluorogenic probe, such as fluorogenic arylsulfates to reveal sulfatases[15,16] or acetoxymethyl ether (AME)-masked probes to detect esterases.[17] Originally, we reported that this assay could distinguish mycobacterial species and strains based on sulfatase activity.[15] More recently, we observed highly conserved esterase activity for *Mtb* complex (MTBC) members —organisms that cause TB.[17] However, we saw far fewer fluorescent bands in this assay than we anticipated based on the *Mtb* genome, and we suspected that our two-carbon (C2) AME probes were hydrolyzed by only a subset of the *Mtb* esterases. Many *Mtb* esterases and lipases, including Culp1, LipC, LipH, LipI, and LipY, prefer longer four-carbon (C4) and eight-carbon (C8) substrates.[11,14,18,19] Therefore, we report herein an expanded probe set with C4 and C8 acyloxymethyl ether derivatives of DDAO, a far-red fluorophore. We validated these probes with a panel of esterases and lipases. We then used these new substrates to reveal esterase activity in lysates from mycobacteria and *Mtb*-infected macrophages.

In our work, much of our probe development has focused on far-red fluorophores that excite above 600 nm (i.e., DDAO[15,17] or DSACO[20]). Cellular autofluorescence and light scattering is minimal in this region of the spectrum, giving far-red fluorophores superior fluorescent properties for imaging in living systems.[21] Therefore, we modified DDAO to create a set of fluorogenic esterase probes (Scheme 1). The archetypical fluorogenic esterase probe is green-fluorescent fluorescein diacetate, but acetate-masked probes are hydrolytically unstable. Chemists have used acyloxymethyl ethers to create esterase probes with improved stability.[22,23] We synthesized AME-masked DDAO substrates through a silver-mediated *O*-

alkylation, as previously described.[17] The C4 butanoylmethyl ether (BME)- and C8 octanoylmethyl ether (OME)-masked substrates were synthesized in good yields under biphasic conditions from DDAO and the corresponding iodomethyl esters. Both reactions produced a mixture of 2- and 7-substituted regioisomers, which were separated by column chromatography. The lower calculated pK_a[24] of the 2-position phenol tautomer favored formation of the 2-substituted product under these reaction conditions. We assigned substrate regiochemistry though heteronuclear single quantum correlation (HSQC) and heteronuclear multiple bond correlation (HMBC) 2D-NMR spectroscopy, as described in the Supporting Information.

We determined the spectral properties of each compound (Table 1 and Figure S1), including absorbance (λ_{abs}) and emission (λ_{em}) maxima, extinction coefficients (ε), and quantum yields (ϕ). Consistent with the DDAO-AME probes,[17] the absorbance maxima of the BME- and OME-masked DDAO compounds were significantly blue-shifted from DDAO. The extinction coefficients of these compounds were also 2- to 3-fold lower compared with the parent compound. All of the 2-substituted regioisomers were nonfluorescent, and the 7-substituted regioisomers retained minimal fluorescence. DDAO-7-BME and DDAO-7-OME had over a 50-fold reduction in quantum yield compared with DDAO. These were also an order of magnitude lower than DDAO-7-AME. We measured the relative fluorescence of the masked compounds using DDAO's excitation and emission settings (λ_{ex} 635 nm, λ_{em} 670 nm); all six exhibited a 650- to 1420-fold reduction in fluorescence compared with DDAO. Because the 2-masked substrates are nonfluorescent, the fluorescence detected with these settings is likely due to trace amounts of DDAO. These data show that the acyloxymethyl ether-masked DDAO probes are excellent "turn-on" substrates.

We assessed probe reactivity with a diverse panel of commercially available esterases and lipases (Figure 1). Heat-killed porcine liver esterase (PLE) did not hydrolyze our substrates, demonstrating that an active enzyme is required for probe cleavage. After 30 min, all of the probes were hydrolyzed by every enzyme, but to varying degrees. As expected, the longer-chain BME- and OME-masked probes were improved lipase substrates compared with the AME-masked probes, but they also retained high esterase reactivity. DDAO-7-BME was a moderately less favorable substrate for this enzyme panel compared with DDAO-2-BME and the two OME-masked probes. Despite their different chain lengths, DDAO-2-BME and DDAO-2-OME displayed nearly identical reactivity profiles. Overall, the longer-chain DDAO-derived probes had improved reactivity compared to the AME-masked probes, highlighting the versatility of these new probes as esterase and lipase substrates.

We further characterized the probes with PLE, determining their kinetic parameters (Figure S2) and detection limits (Figure S3). All six fluorogenic probes were good PLE substrates with Michaelis constants (K_M) ranging from 3 to 9 μM. The catalytic efficiency (k_{cat}/K_M) ranged from 0.2 $\mu M^{-1}s^{-1}$ (DDAO-2-AME) to 0.7 $\mu M^{-1}s^{-1}$ (DDAO-2-OME). The AME-masked probes were the least sensitive for PLE detection (25 pg/mL), while DDAO-2-BME, DDAO-7-OME, and DDAO-2-OME were 10-fold more sensitive (2.5 pg/mL). DDAO-7-BME had intermediate sensitivity (5 pg/mL). Additionally, the new probes had improved hydrolytic stability, with ≥90% of each probe remaining after 60 h (Table S1, Figure S4).

Fluorogenic esterase probes are common reagents for live-cell imaging.[25] We evaluated our new probes with a human osteosarcoma cell line using confocal fluorescence microscopy. All of our DDAO-derived probes were rapidly internalized and hydrolyzed by intracellular esterases to generate DDAO-stained cells (Figure S5). The AME- and BME-masked probes produced more DDAO fluorescence than the OME-masked probes at the same concentration. Therefore, DDAO acyloxymethyl ethers are a far-red alternative to fluorescein derivatives for live-cell imaging.

Next, we used these six probes to profile *Mtb* esterase and lipase activities. Many of these enzymes are secreted[11,12] or cellwall-associated,[9,26] making them good targets for assessing whole-cell esterase activity. We found that all six probes were hydrolyzed by live *Mtb* mc^{2}6020, an auxotrophic strain derived from the virulent H37Rv lab strain (Figure S6).[27] However, this whole-cell assay did not indicate whether the new probes could reveal esterases missed by our AME-masked probes. We used a native PAGE-based assay to profile esterase and lipase activity patterns, as previously described.[15–17] We evaluated lysates from *M. smegmatis, M. marinum, Mtb* mc^{2}6020, and *M. bovis* (BCG), an attenuated vaccine strain (Figure 2a). Overall, the four species displayed different esterase activity patterns, but with high similarity between *Mtb* mc^{2}6020 and *M. bovis* (BCG), two members of the MTBC. Despite biochemical evidence that many *Mtb* esterases prefer longer-chain substrates,[11,14,18,19] DDAO-7-AME revealed the greatest number of *Mtb* esterases. A subset of these enzymes were revealed by the BME-masked probes, with the absent bands likely attributable to esterases preferring C2 esters. The OME-masked probes were activated by the same *Mtb* enzymes as the BME probes but revealed an additional band not detected with the shorter-chain probes. Interestingly, this band was present in the *Mtb* lysate and not in the BCG lysate. The differences revealed by these probes highlight the benefits of using probes of varying chain lengths in order to track different enzyme sub-classes. These results also demonstrate the power of fluorogenic probes coupled with the in-gel activity-based assay for observing enzyme differences in closely related species.

Because we previously observed highly conserved esterase activity patterns for MTBC members,[17] we were intrigued by the *Mtb*-specific esterase band revealed by the OME probes. We excised this band and subjected it to in-gel tryptic digestion and protein identification by mass spectrometry. The gel slice contained peptides corresponding to Culp1 (Rv1984c), a secreted cutinase-like protein with esterase activity (Table S2).[28,29] The gene encoding Culp1 lies within the region of deletion 2 (RD2), a genomic region that is deleted in *M. bovis* (BCG) sub-strains but retained in *Mtb*.[7,30,31] This genomic difference accounts for the band's absence in *M. bovis* (BCG) lysate.

We used an *Mtb* CDC1551 transposon mutant to confirm that the fluorescent signal was produced through Culp1-mediated hydrolysis. The OME-specific band was present in lysate from the wild type *Mtb* CDC1551 but absent in the Culp1 transposon mutant (Figure 2b). We also examined conditioned medium from *Mtb* mc^{2}6020. We observed two strongly fluorescent bands at a lower apparent molecular weight than the Culp1 whole-cell lysate band (Figure 2c). Culp1 contains a signal sequence that is cleaved upon export,[32] and we reasoned that this post-translational modification could result in greater protein mobility in-gel. To test this hypothesis, we excised these bands and identified Culp1 peptides in both.

Sequence coverage for both bands began at the *N*-terminus of the cleaved, secreted protein (Table S2).[32] Therefore, Culp1 is active both within bacilli and upon secretion. This result highlights the utility of fluorogenic probes for detecting *Mtb* esterases in both lysates and conditioned medium.

Culp1 is one of the best-studied *Mtb* esterases. Recombinant Culp1 was characterized as maximally active with a C4 substrate by West and co-workers,[11] but Schué *et al.* found that it was 86-times more active with a C8 substrate over a C4 substrate.[18] Our results indicate that Culp1 prefers C8 substrates, which agrees with the findings of Schué *et al.* Culp1 induces alveolar epithelial cell apoptosis,[33] suggesting that it may contribute to *Mtb* pathogenesis by facilitating mycobacterial dissemination. Because it is an immunodominant RD antigen, Culp1 has been explored as a potential candidate for an improved TB vaccine.[29,34] Immunization with recombinant Culp1 provided partial protection against TB,[29] and supplementing the BCG vaccine with Culp1 and other RD antigens enhanced the vaccine's efficacy in mice.[34] The ability to track Culp1 activity using OME-masked fluorogenic substrates could benefit future investigations of this clinically relevant esterase.

Next, we evaluated lysates from *Mtb* mc^{2}6020-infected murine macrophages (Figure 2d). Mock-infected macrophages were prepared in tandem to compare host cell esterase activity. In mock-infected macrophage lysates, DDAO-7-BME revealed the greatest number of esterases, while DDAO-7-OME revealed the fewest. *Mtb*-infected samples displayed esterase bands originating from both the host and the pathogen. Notably, a subset of the *Mtb* esterase bands could be distinguished from those originating from host cells based on their migration patterns. For example, macrophage-associated esterases generally appeared in the top portion of the gel, while *Mtb* esterases were more prominent in the lower quadrant. DDAO-7-OME provided the clearest *Mtb* banding patterns in these complex lysates and revealed Culp1 activity in *Mtb*-infected macrophages. These results demonstrate that our assay platform can track esterase activity in mixed cell populations without interference from host enzymes. We anticipate that this type of assay will be useful for analyzing esterase activity in other host–pathogen models, including *Mtb*-infected animal tissues or patient-derived samples.

In conclusion, we synthesized and characterized C4 and C8 acyloxymethyl ether-masked fluorogenic probes from the far-red fluorophore DDAO. These probes were "turn-on" substrates with superior stability and esterase reactivity compared with our previously reported C2-masked probes. This expanded set is a powerful toolbox for uncovering substrate preferences, quantifying esterase activities, and live-cell microscopy. We used our DDAO-derived probes to examine *Mtb* esterases and lipases in whole cells and in native PAGE-resolved lysates. The OME-masked probes revealed a key difference in esterase activity between *Mtb* and *M. bovis* (BCG), two closely related species. The *Mtb*-specific band was identified as Culp1, a clinically relevant secreted esterase. The OME-masked probes were also better for distinguishing mycobacterial esterases from host cell esterases in *Mtb*-infected macrophage lysates. Overall, our probes are long-chain, far-red fluorogenic substrates that can be used for detecting and tracking esterase and lipase activities in a wide range of assay formats.

METHODS

Details of experimental procedures are provided in the Supporting Information.

Supplementary Material

Refer to Web version on PubMed Central for supplementary material.

ACKNOWLEDGMENTS

We are grateful to our collaborators L. Lavis (Janelia Research Campus/HHMI) and J. Johnson (Butler University) for productive discussions. We thank M. Harriff and the D. Lewinsohn laboratory (OHSU) for assistance with our BSL-3 experiments. The W. Jacobs laboratory (Albert Einstein College of Medicine and HHMI) kindly shared their *Mtb* $mc^2$6020 auxotrophic strain. BEI Resources (NIAID, NIH) supplied the *Mtb* CDC1551 strains, both wild type and the transposon mutant 2944 (MT2037, Rv1984c; NR-18745). We thank J. Doh for her assistance with live-cell imaging. HRMS data were collected on Portland State University's ThermoElectron LTQ-Orbitrap Discovery (NSF instrument grant 0741993). Funding for this research was generously provided by the Knight Cancer Institute at OHSU, the Collins Medical Trust, and the Medical Research Foundation of Oregon. S.R.L. was supported by an NIH T32 training grant (T32-AI07472).

REFERENCES

1. World Health Organization. (2015) Global Tuberculosis Report 2015.
2. Tufariello JM, Chan J, and Flynn JL (2003) Latent tuberculosis: Mechanisms of host and bacillus that contribute to persistent infection. Lancet Infect. Dis 3, 578–590. [PubMed: 12954564]
3. Deb C, Daniel J, Sirakova TD, Abomoelak B, Dubey VS, and Kolattukudy PE (2006) A novel lipase belonging to the hormone-sensitive lipase family induced under starvation to utilize stored triacylglycerol in *Mycobacterium tuberculosis*. J. Biol. Chem 281, 3866–3875. [PubMed: 16354661]
4. Low KL, Rao PS, Shui G, Bendt AK, Pethe K, Dick T, and Wenk MR (2009) Triacylglycerol utilization is required for regrowth of in vitro hypoxic nonreplicating *Mycobacterium bovis* bacillus Calmette-Guerin. J. Bacteriol 191, 5037–5043. [PubMed: 19525349]
5. Daniel J, Maamar H, Deb C, Sirakova TD, and Kolattukudy PE (2011) *Mycobacterium tuberculosis* uses host triacylglycerol to accumulate lipid droplets and acquires a dormancy-like phenotype in lipid-loaded macrophages. PLoS Pathog. 7, e1002093. [PubMed: 21731490]
6. Brust B, Lecoufle M, Tuaillon E, Dedieu L, Canaan S, Valverde V, and Kremer L (2011) *Mycobacterium tuberculosis* lipolytic enzymes as potential biomarkers for the diagnosis of active tuberculosis. PLoS One 6, e25078. [PubMed: 21966416]
7. Cole ST, Brosch R, Parkhill J, Garnier T, Churcher C, Harris D, Gordon SV, Eiglmeier K, Gas S, Barry CE, Tekaia F, Badcock K, Basham D, Brown D, Chillingworth T, Connor R, Davies R, Devlin K, Feltwell T, Gentles S, Hamlin N, Holroyd S, Hornsby T, Jagels K, Krogh A, McLean J, Moule S, Murphy L, Oliver K, Osborne J, Quail MA, Rajandream MA, Rogers J, Rutter S, Seeger K, Skelton J, Squares R, Squares S, Sulston JE, Taylor K, Whitehead S, and Barrell BG (1998) Deciphering the biology of *Mycobacterium tuberculosis* from the complete genome sequence. Nature 393, 537–544. [PubMed: 9634230]
8. Hotelier T, Renault L, Cousin X, Negre V, Marchot P, and Chatonnet A (2004) ESTHER, the database of the alpha/beta-hydrolase fold superfamily of proteins. Nucleic Acids Res. 32, D145–147. [PubMed: 14681380]
9. Lun S, and Bishai WR (2007) Characterization of a novel cell wall-anchored protein with carboxylesterase activity required for virulence in *Mycobacterium tuberculosis*. J. Biol. Chem 282, 18348–18356. [PubMed: 17428787]
10. Sultana R, Vemula MH, Banerjee S, and Guruprasad L (2013) The PE16 (Rv1430) of *Mycobacterium tuberculosis* is an esterase belonging to serine hydrolase superfamily of proteins. PLoS One 8, e55320. [PubMed: 23383323]

11. West NP, Chow FM, Randall EJ, Wu J, Chen J, Ribeiro JM, and Britton WJ (2009) Cutinase-like proteins of *Mycobacterium tuberculosis*: Characterization of their variable enzymatic functions and active site identification. FASEB J. 23, 1694–1704. [PubMed: 19225166]
12. Chen L, Dang G, Deng X, Cao J, Yu S, Wu D, Pang H, and Liu S (2014) Characterization of a novel exported esterase Rv3036c from *Mycobacterium tuberculosis*. Protein Expression Purif. 104C, 50–56.
13. Dang G, Chen L, Li Z, Deng X, Cui Y, Cao J, Yu S, Pang H, and Liu S (2015) Expression, purification and characterisation of secreted esterase Rv2525c from *Mycobacterium tuberculosis*. Appl. Biochem. Biotechnol 176, 1–12. [PubMed: 25869294]
14. Delorme V, Diomande SV, Dedieu L, Cavalier JF, Carriere F, Kremer L, Leclaire J, Fotiadu F, and Canaan S (2012) MmPPOX inhibits *Mycobacterium tuberculosis* lipolytic enzymes belonging to the hormone-sensitive lipase family and alters mycobacterial growth. PLoS One 7, e46493. [PubMed: 23029536]
15. Beatty KE, Williams M, Carlson BL, Swarts BM, Warren RM, van Helden PD, and Bertozzi CR (2013) Sulfatase-activated fluorophores for rapid discrimination of mycobacterial species and strains. Proc. Natl. Acad. Sci. U. S. A 110, 12911–12916. [PubMed: 23878250]
16. Smith EL, Bertozzi CR, and Beatty KE (2014) An expanded set of fluorogenic sulfatase activity probes. ChemBioChem 15, 1101–1105. [PubMed: 24764280]
17. Tallman KR, and Beatty KE (2015) Far-red fluorogenic probes for esterase and lipase detection. ChemBioChem 16, 70–75. [PubMed: 25469918]
18. Schué M, Maurin D, Dhouib R, N'Goma JCB, Delorme V, Lambeau G, Carriere F, and Canaan S (2010) Two cutinase-like proteins secreted by *Mycobacterium tuberculosis* show very different lipolytic activities reflecting their physiological function. FASEB J. 24, 1893–1903. [PubMed: 20103719]
19. Lukowski JK, Savas CP, Gehring AM, McKary MG, Adkins CT, Lavis LD, Hoops GC, and Johnson RJ (2014) Distinct substrate selectivity of a metabolic hydrolase from *Mycobacterium tuberculosis*. Biochemistry 53, 7386–7395. [PubMed: 25354081]
20. Levine SR, and Beatty KE (2016) Synthesis of a far-red fluorophore and its use as an esterase probe in living cells. Chem. Commun. (Cambridge, U. K.) 52, 1835–1838.
21. Weissleder R, and Ntziachristos V (2003) Shedding light onto live molecular targets. Nat. Med 9, 123–128. [PubMed: 12514725]
22. Leroy E, Bensel N, and Reymond JL (2003) A low background high-throughput screening (HTS) fluorescence assay for lipases and esterases using acyloxymethylethers of umbelliferone. Bioorg. Med. Chem. Lett 13, 2105–2108. [PubMed: 12798314]
23. Lavis LD, Chao TY, and Raines RT (2011) Synthesis and utility of fluorogenic acetoxymethyl ethers. Chem. Sci 2, 521–530. [PubMed: 21394227]
24. Calculator plugins for Marvin were used for structure property prediction and calculation. (2015) Marvin, 15.3.30 ed., ChemAxon http://chemaxon.com.
25. Johnson I, and Spence MTZ (2010) Molecular Probes Handbook: A Guide to Fluorescent Probes and Labeling Technologies, 11th ed., Life Technologies Corportation.
26. Shen G, Singh K, Chandra D, Serveau-Avesque C, Maurin D, Canaan S, Singla R, Behera D, and Laal S (2012) LipC (Rv0220) is an immunogenic cell surface esterase of *Mycobacterium tuberculosis*. Infect. Immun 80, 243–253. [PubMed: 22038913]
27. Sambandamurthy VK, Derrick SC, Jalapathy KV, Chen B, Russell RG, Morris SL, and Jacobs WR Jr. (2005) Long-term protection against tuberculosis following vaccination with a severely attenuated double lysine and pantothenate auxotroph of *Mycobacterium tuberculosis*. Infect. Immun 73, 1196–1203. [PubMed: 15664964]
28. Weldingh K, Rosenkrands I, Jacobsen S, Rasmussen PB, Elhay MJ, and Andersen P (1998) Two-dimensional electrophoresis for analysis of *Mycobacterium tuberculosis* culture filtrate and purification and characterization of six novel proteins. Infect. Immun 66, 3492–3500. [PubMed: 9673225]
29. Grover A, Ahmed MF, Verma I, Sharma P, and Khuller GK (2006) Expression and purification of the *Mycobacterium tuberculosis* complex-restricted antigen CFP21 to study its immunoprophylactic potential in mouse model. Protein Expression Purif. 48, 274–280.

30. Mahairas GG, Sabo PJ, Hickey MJ, Singh DC, and Stover CK (1996) Molecular analysis of genetic differences between *Mycobacterium bovis* BCG and virulent *M. bovis*. J. Bacteriol 178, 1274–1282. [PubMed: 8631702]

31. Behr MA, Wilson MA, Gill WP, Salamon H, Schoolnik GK, Rane S, and Small PM (1999) Comparative genomics of BCG vaccines by whole-genome DNA microarray. Science 284, 1520–1523. [PubMed: 10348738]

32. Malen H, Berven FS, Fladmark KE, and Wiker HG (2007) Comprehensive analysis of exported proteins from *Mycobacterium tuberculosis* H37Rv. Proteomics 7, 1702–1718. [PubMed: 17443846]

33. Vir P, Gupta D, Agarwal R, and Verma I (2014) Interaction of alveolar epithelial cells with CFP21, a mycobacterial cutinase-like enzyme. Mol. Cell. Biochem 396, 187–199. [PubMed: 25091806]

34. Kalra M, Grover A, Mehta N, Singh J, Kaur J, Sable SB, Behera D, Sharma P, Verma I, and Khuller GK (2007) Supplementation with RD antigens enhances the protective efficacy of BCG in tuberculous mice. Clin. Immunol 125, 173–183. [PubMed: 17766185]

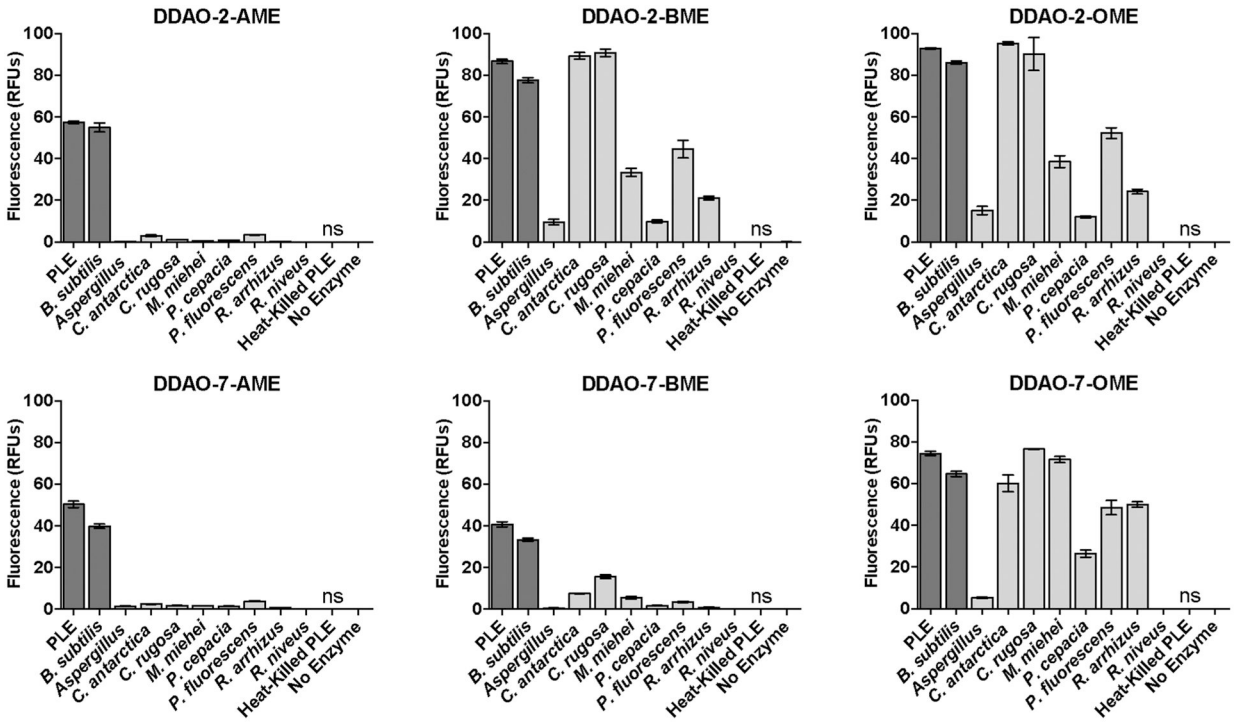

Figure 1.

DDAO-based fluorogenic probes are versatile esterase and lipase substrates. Fluorescence generation by esterases (dark gray bars) and lipases (light gray bars) is given in relative fluorescence units (RFUs). All unlabeled responses are statistically significant ($P < 0.01$), and those labeled “ns” were not significant compared to the enzyme-free control. Error bars represent one standard deviation ($n = 4$).

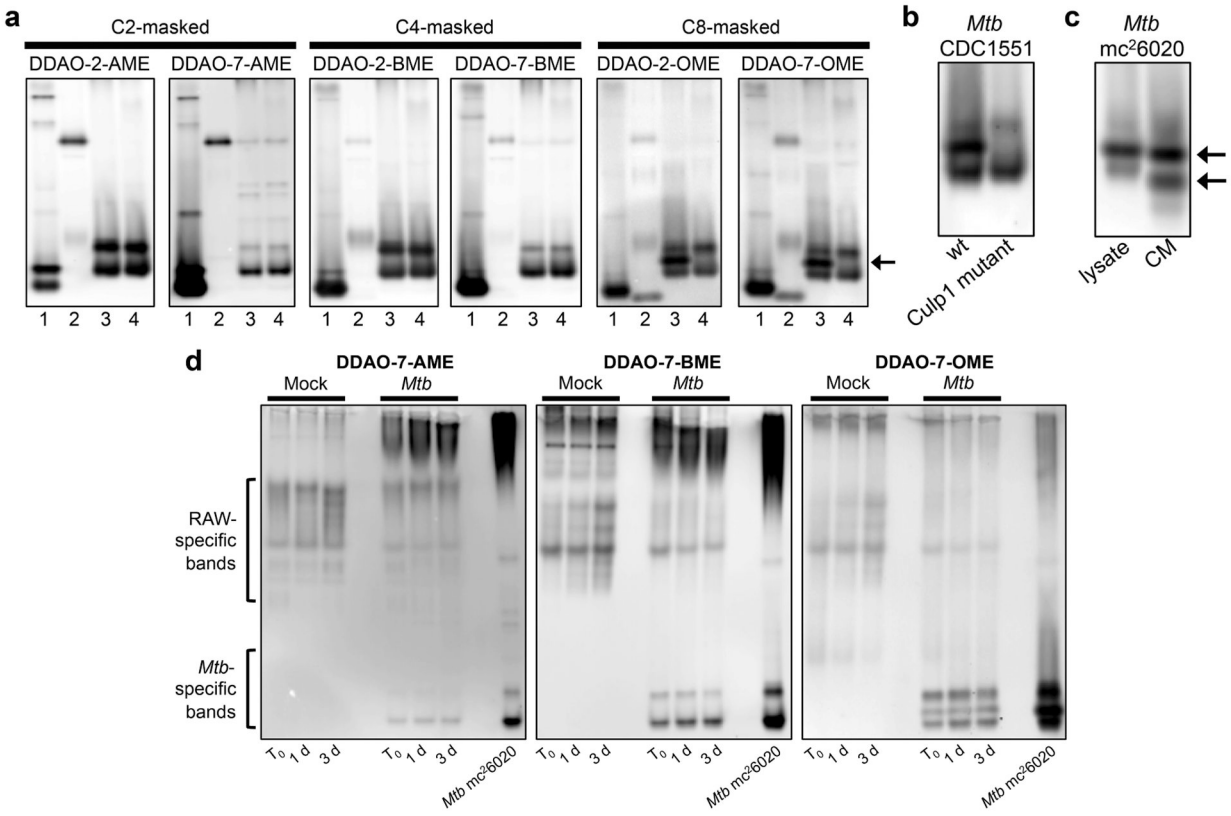

Figure 2.

DDAO-derived fluorogenic probes reveal mycobacterial esterases and lipases in native PAGE-resolved lysates. (a) Lysates from (1) *M. smegmatis*, (2) *M. marinum*, (3) *Mtb* mc^{2}6020, and (4) *M. bovis* (BCG) were examined. The arrow highlights an *Mtb*-specific band revealed by the OME probes. (b) Lysates from *Mtb* CDC1551 wild type (wt) and a Culp1 transposon mutant confirmed that the *Mtb*-specific band corresponds to Culp1 activity. (c) Whole-cell lysate and conditioned medium (CM) from *Mtb* mc^{2}6020 both displayed Culp1 activity. Arrows indicate bands in the CM identified as Culp1 by mass spectrometry-based proteomics. (d) *Mtb*-infected RAW macrophages were collected and lysed immediately after the 4 h infection (T_0), 1 day post-infection, or 3 days post-infection. Mock-infected macrophage lysates and *Mtb* mc^{2}6020 lysates were analyzed for comparison.

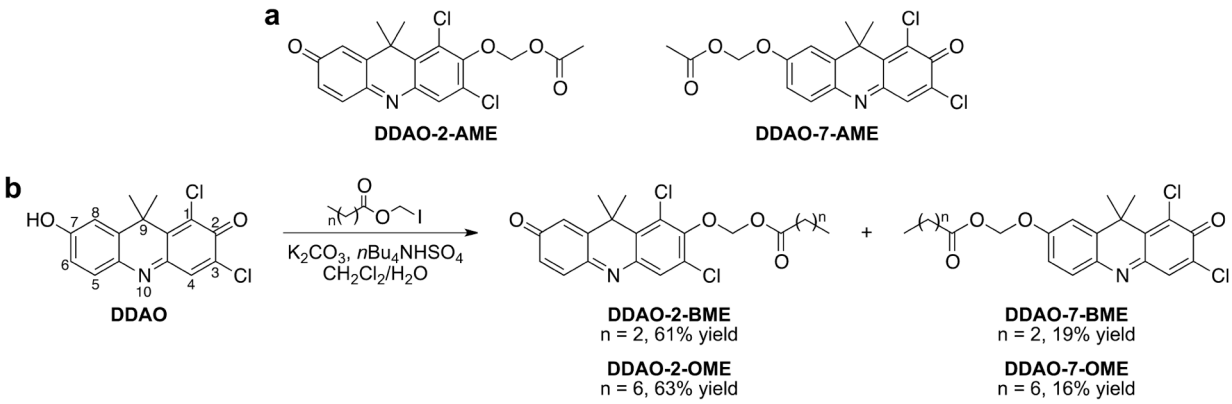

Scheme 1.

Structures of DDAO-Derived Fluorogenic Esterase Probes: (a) Previously Reported DDAO-AME Probes[17] and (b) Synthesis of Longer-Chain DDAO-Acyloxymethyl Ethers and Illustration of the DDAO Numbering Scheme

Table 1.

Spectral Properties of DDAO and DDAO-Derived Fluorogenic Probes in 10 mM HEPES (pH 7.3)

compound	λ_{abs} (nm)	λ_{em} (nm)	ε ($M^{-1}cm^{-1}$)	ϕ[a]	fluorescence decrease[b]
DDAO	646	659	36 000	0.39	
DDAO-2-AME	395		11 000		1420-fold
DDAO-7-AME	465	625	4900	0.07	890-fold
DDAO-2-BME	400		13 000		1015-fold
DDAO-7-BME	453	613	14 000	0.006	1180-fold
DDAO-2-OME	392		21 000		890-fold
DDAO-7-OME	451	614	23 000	0.007	650-fold

[a]The fluorescence quantum yields were measured at 25 °C using oxazine 1 (ϕ = 0.15 in EtOH) or fluorescein (ϕ = 0.89 in 0.1 M NaOH) as reference standards.

[b]The fluorescence decrease was calculated as the ratio of DDAO fluorescence and fluorogenic probe fluorescence at the same concentration (λ_{ex} 635 nm, λ_{em} 670 nm).